Transactions of the Materials Research Society of Japan 33[1] 27-30 (2008)

Microstructures related to the ferroelectric properties in $BiFeO_3$-$BaTiO_3$

S. Kitagawa, Y. Horibe[1], K. Yoshii[2], M. Suzuki[3], Y. Noguchi[3], S. Nishihara, Y. Hosokoshi and S. Mori
Osaka Prefecture University, Sakai, Osaka 599-853, Japan
[1]Rutgers University, Piscataway, NJ, 08854, U.S.A
[2]Japan Atomic Agency, Hyogo 679-5148, Japan
[3]Research Center for Advanced Science Technology, The University of Tokyo, Tokyo 153-8904, Japan

Microstructures related to the ferroelectric (FE) properties in (1-x)$BiFeO_3$-x$BaTiO_3$ were examined mainly by a transmission electron microscopy, in combination with conventional magnetic and dielectric measurements. It was found that macroscopic-sized FE domain structures in $BiFeO_3$ changed into fine FE microstructures with the 20-30nm size in the x=0.25 compound, as the $BaTiO_3$ concentration (x) was increased. In addition, we found characteristic tweed-like contrast due to the strain field in the x=0.33 compound at room temperature. We carefully investigated a spatial distribution of the FE microdomains in the x=0.25 compound by obtaining real-space images and determined the spatial configuration of the spontaneous polarization in each FE microdomains.

Key words: ferroelectric domain, multi-ferroic material, transmission electron microscopy

There has been a recent surge of interest in the physics and applications of multiferroic materials. Multiferroic materials have coupled electric, magnetic and/or structural order parameters that result in simultaneous ferromagnetic, ferroelectric and ferro-elastic behavior. Coupling between the spontaneous polarization and spontaneous magnetization leads to magnetoelectric effects, in which the magnetization can be controlled by an applied electric field and vice versa. Recently it has been revealed that the magnetic and electric degrees of freedom can allow both charge and spin to be controlled by applied electric or magnetic field [1-5]. Several composite materials such as $BaTiO_3$-$CoFe_2O_4$ have been reported to show magnetoelectric effect at room temperature [6]. However there are few materials which exhibit the coupling between magnetic and electric order parameters at room temperature.

$BiFeO_3$ undergoes a ferroelectric phase transition around T_c~1100K and shows a ferroelectric polarization of 6.1 $\mu C/cm^2$ at room temperature [7]. Simultaneously this ferroelectric transition accompanies with the structural phase transition to the rhombohedral one with the space group of *R3c* and results in the ferroelectric polarization along the [111] direction. Note that the crystal structure in the high-temperature paraelectric phase has not been conclusively determined. As the temperature was decreased from 1100K, an antiferromagnetic transition takes place around T_N~640K. It has been known that $BiFeO_3$ is characterized by the coexisting state between ferroelectricity and antiferromagnetism at room temperature [7-9]. The magnetic structure is regarded as the G-type antiferromagnetic (AF) structure in the first approximation. Practically the G-type AF structure is modified by the long-range modulation with a cycloidal spiral of λ=62nm length along the [110] direction [10]. $BiFeO_3$ has been reported to show the liner magneto-electric effect, in which week ferromagnetic ordering was induced and ferroelectric polarization was enhanced by applied magnetic field. Recently, Wang et al. found the emergence of large polarization of 63.2 $\mu C/cm^2$ in $BiFeO_3$ thin films with the tetragonal symmetry (*P4mm*) at room temperature [11]. This suggests that the crystal structure has a close relation to how large the polarization appears in $BiFeO_3$.

According to a previous work by Kumar et al., it has been reported that $BiFeO_3$ forms a solid solution with a number of other oxides with the perovskite structure such as $BaTiO_3$, $PbTiO_3$ and $SrTiO_3$ [12-14]. In the case of $BiFeO_3$-$BaTiO_3$ solid solutions, it was revealed that $BiFeO_3$-$BaTiO_3$ compounds exhibit structural phase transition with respect to the $BaTiO_3$ compositional range (x) at room temperature [12]. In the (1-x)$BiFeO_3$-x$BaTiO_3$ ($0.0<x<0.3$) compounds, the crystal structure is identified as the rhombohedral one with the *R3c* space group at room temperature. On the other hand, the (1-x)$BiFeO_3$-x$BaTiO_3$ ($0.96<x<1.0$) compounds has a tetragonal structure and in between the crystal structure is cubic. As the $BaTiO_3$ composition (x) is increased, the ferroelectric Curie temperature decreases and the value of dielectric constant increases. These results suggest that there are some relationship between structural changes and dielectric properties in the $BiFeO_3$-$BaTiO_3$ solid solutions. Thus, we investigated systematically changes of microstructures related to the ferroelectric properties in the $BiFeO_3$-$BaTiO_3$ solid solutions mainly by the transmission electron microscopy, in combination with the conventional magnetic and dielectric measurements.

We prepared polycrystalline samples of (1-x)$BiFeO_3$-x$BaTiO_3$ with x=0.0, 0.20, 0.25 and 0.33 in air by the conventional solid-state reaction method. The procedure of the samples was as follows. The starting materials were Bi_2O_3, Fe_2O_3 and $BaTiO_3$. The initial mixtures were well ground and then pressed into a pellet. The pellets were preheated for 30 h twice at 1123 K and 1153 K, respectively. Subsequently, the preheated

samples were sintered for 72 h in air at 1173 K. Finally, the obtained samples were annealed at 993 K for 48 h. We checked crystal structures of the obtained samples by x-ray diffraction method. The magnetic measurements were carried out in a SQUID magnetometer at room temperature. For the TEM observation, we prepared some thin-film specimens by the Ar-ion thinning method. The TEM experiments were carried out in a JEM-2010 TEM operating at 200 kV. It should be noted that polycrystalline samples prepared by several different sintering temperatures were measured by both x-ray diffraction and dielectric-constant measurements and the same results in these samples were obtained. Therefore we chose 30-50 K lower than their melting temperatures in order to optimize the grain size for the TEM observation.

Figure 1(a) displays variation of magnetization (M) as a function of the applied magnetic field (H) between -10 T and 10 T in the (1-x)$BiFeO_3$-x$BaTiO_3$ compounds with x=0.20 and 0.33. It has been reported that $BiFeO_3$ (x=0.0) with the AF ordering shows the liner response of the magnetization to the applied magnetic field [15]. On the other hand, as x was increased, it is found that the so-called magnetic hysteresis response of the magnetization to the applied

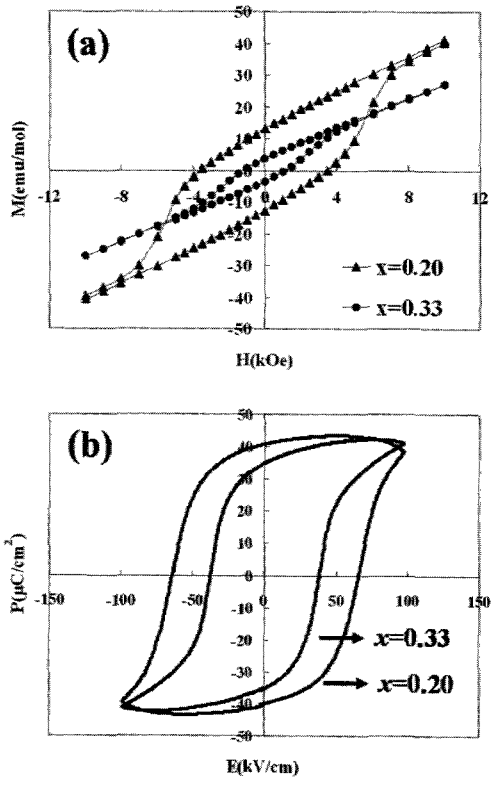

Fig.1. (a) M-H hysteresis curves (b) P-E hysteresis curves in x=0.20 and x=0.33 compounds at room temperature.

magnetic field can be seen in the x=0.20 and 0.33 compounds, as understood evidently in Fig. 1(a). This means that week ferromagnetic moment appears in the x=0.20 and 0.33 compounds, which is consistent with the observed magnetic hysteresis curve in the (1-x)$BiFeO_3$-x$BaTiO_3$ (x=0.30) thin film [13]. Figure 1(b) shows variation of the spontaneous polarization (P_s) as a function of the applied electric field (E) between -100 kV/cm and 100 kV/cm at room temperature. As clearly shown in Fig. 1(b), the ferroelectric hysteresis curves can be observed in the x=0.20 and 0.33 compounds. Note that the values of the spontaneous polarization are about 40 $\mu C/cm^2$ and 35 $\mu C/cm^2$, respectively. As evident in Fig. 1, the magnetic and ferroelectric hysteresis curves clearly demonstrate the presence of the coexisting state between ferroelectric and ferromagnetic orderings in the x=0.20 and 0.33 compounds. Namely, the x=0.20 and 0.33 compounds can be characterized as the *multiferroic* materials.

$BiFeO_3$ has a rhombohedrally distorted perovskite-type structure with the space group *R3c*. This rhombohedral structure consists of the cooperative rotation of FeO_6 octahedra along the [111] direction, in addition to the polar displacements of Bi, Fe and O ions along the [111] direction. To clarify changes of the crystal structures by the increase of x in (1-x)$BiFeO_3$-x$BaTiO_3$, we carefully investigated various electron diffraction patterns at room temperature. Figure 2 shows the electron diffraction patterns in (1-x)$BiFeO_3$-x$BaTiO_3$ with (a) x=0.0 ($BiFeO_3$), (b) 0.20, (c) 0.25 and 0.33, respectively. Note that the electron beam incidence is parallel to the [1-10] direction. As indicated by arrows in Figs. 2(a), 2(b) and 2(c), superlattice reflection spots at 1/2 1/2 1/2-type positions can be clearly seen, in addition to the fundamental spots due to the cubic perovskite-type structure. As understood by comparing intensities of the superlattice reflection spots at 1/2 1/2 1/2-type positions in Figs. 2(a), 2(b) and 2(c), intensities in $BiFeO_3$ are much stronger than those in the x=0.20 and x=0.25 compounds. It should be noted that the rhombohedral distortion in these compounds is characterized by the presence of the superlattice reflection spots at 1/2 1/2 1/2-type positions. These imply that the rhombohedral distortion in the x=0.20 and 0.25 compounds is much smaller than that in $BiFeO_3$. That is, it is suggested that the magnitudes of the displacements of Bi, Fe and O ions along [111] direction decrease by partially substituting $BaTiO_3$ for $BiFeO_3$. Because these displacements give rise to the spontaneous polarization in the rhombohedral phase of $BiFeO_3$, the values (40 μ/cm^2 and 35 μ/cm^2) of the spontaneous polarization in the x=0.20 and 0.33 compounds are relatively smaller than that predicted in the theoretical calculation in $BiFeO_3$ [9]. On the other hand, no superlattice reflection spot at 1/2 1/2 1/2-type positions can be seen in the x=0.33 compound, as can be understood in Fig. 2(d). This means that the rhombohedral distortion disappears and the x=0.33 compound should change into the cubic structure, as

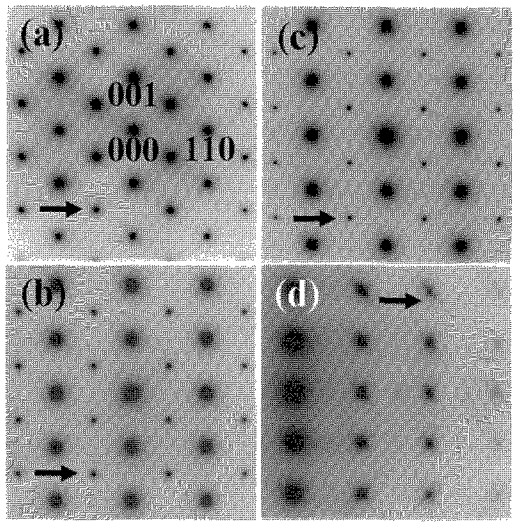

Fig.2. [1-10]-zone axis electron-diffraction patterns at room temperature in (a) x=0.0 ($BiFeO_3$), (b) x=0.20, (c) x=0.25 and (d) x=0.33 compounds, respectively.

reported in the previous work [12]. On the other hand, we can see clearly characteristic diffuse streak elongating from the fundamental spots, as indicated by an arrow in Fig. 2(d). It is necessary to clarify the microstructures giving rise to the characteristic diffuse streak found in the x=0.33 compound.

Thus, we carefully investigated changes of the microstructures related to the ferroelectric properties by obtaining the real-space images at room temperature in (1-x)$BiFeO_3$-x$BaTiO_3$. Figure 3 displays the dark-field images obtained by using the 111 fundamental reflection spots. Because the x=0.0 compound has a rhombohedrally distorted structure, large rhombohedral twin structures can be seen, as shown in Fig. 3(a). Note that the rhombohedral twin structures correspond to the ferroelectric (FE) domain structures in $BiFeO_3$ [16]. Figures 3(b) and 3(c) exhibit the microstructures related to the ferroelectric properties in the x=0.20 and 0.25 compounds, respectively. As x was increased, it is found that the average size of the FE domains is reduced and the size can be estimated to be approximately 20~30 nm in the x=0.25 compound. In addition, the boundaries between the adjacent domains are very vague in the x=0.25 compound. As can be understood from Fig. 2, the rhombohedral distortion is reduced by partial substitution of $BaTiO_3$ for $BiFeO_3$. The reduction of the rhombohedral distortion will lead to the reduction of the strain relaxation energy. As a result, unlike in $BiFeO_3$ (Fig.3(a)), the rhombohedral distortion does not necessary produce sharp boundaries nor large domain structures as shown in Fig. 3(c) of the x=0.25 compound. On the contrary, in the case of the x=0.33 compound, as displayed in Fig. 2(d), there are no satellite reflection spots at the 1/2 1/2 1/2-type positions, which are closely related to the rhombohedral distortion. Figure 3(d) is a dark-filed image in the x=0.33 compound. We can not see any indication of the domain

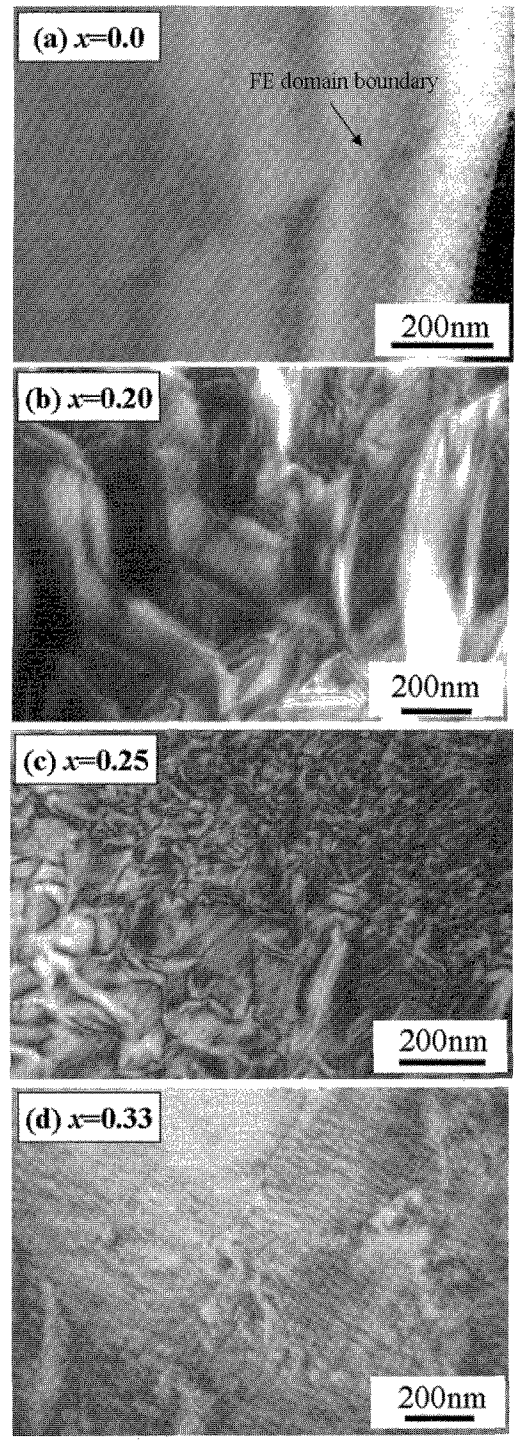

Fig.3. Dark-field images taken using 111 fundamental spot in (a) x=0.0, (b) x=0.20, (c) x=0.25 and (d) x=0.33, respectively.

structures related to the rhombohedral distortion in Fig. 3(d). On the other hand, it is found that there appears characteristic tweed-like contrast, as shown in Fig. 3(d). It should be noted that the tweed-like contrast is often seen in the precursor state just above the 1st order structural phase transition temperature and characterized as the strain-field contrast originating from the

coexisting state due to the emergence of the second phase in the parent phase [17]. From the fact that the tweed-like contrast found in the x=0.33 compound is very similar to that in alloys showing the 1st order transition, it is suggested that the state in the x=0.33 compound should be characterized by the coexisting state. The strain-field due to the coexisting state gives rise to the characteristic diffuse streak elongating from the fundamental spots, as shown in Fig. 2(d).

The spatial distribution of the spontaneous polarization in each FE domains was thoroughly examined by obtaining various dark-field images with the help of the failure of the Friedel's law [18, 19]. Figures 4(a) and 4(b) show a domain structure related to the FE properties in the x=0.25 compound at room temperature. Based on the fact that the spontaneous polarization appears along the [111] direction, we tried to analyze the spatial distribution of the spontaneous polarization in the each FE domains in the x=0.25 compound. Figure 4(c) is a schematic description of the spatial configuration of the spontaneous polarization.

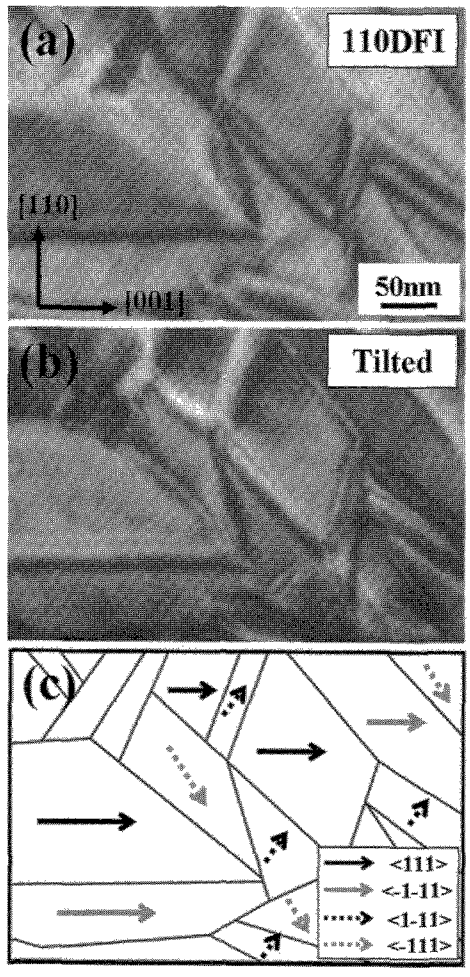

Fig.4. (a), (b) FE domains in the x=0.25 compound at room temperature. (c) Schematic description of the spatial configuration of the spontaneous polarization. The arrows show the direction of the spontaneous polarization in each FE domains. Note that 110DFI in (a) denotes a dark-field image obtained by using the 110 reflection spot. On the contrary, the image (b) is obtained by slightly tilting the sample from the diffraction condition of (a).

In summary, we clarified the microstructures related to the FE properties in (1-x)$BiFeO_3$-x$BaTiO_3$ by TEM experiments. It is found that the rhombohedral distortion disappears in the vicinity of the x=0.33 compound at room temperature. We revealed that the FE domains in $BiFeO_3$ are fragile and changed into finely mixed state consisting of the FE domains with the various directions of the spontaneous polarization by increasing the $BaTiO_3$ concentration (x) in (1-x)$BiFeO_3$-x$BaTiO_3$. In addition, the (1-x)$BiFeO_3$- x$BaTiO_3$ compounds should be good candidates to realize multifunctional devices because of the coexistence of the ferroelectric and ferromagnetic orderings at room temperature.

Acknowledgement

This work was supported by Grant-in-Aid for Scientific Research on Priority Areas "Novel States of Matter Induced by Frustration" (19052002) from Ministry of Education, Culture, Sports, Science and Technology. One of the authors (S.M) was supported partially by the Murata Scientific Foundation.

References

[1]M. Figbig, T. Lottermoser, D. Frohlich, A.V. Golstev and R. V. Pisarev, Nature ***419***, 818-821 (2002).
[2]T. Kimura, et al., Nature ***426***, 55-58 (2003)
[3]N. A. Spaldin and M. Fiebig, Science ***309***, 391-392 (2005).
[4]Th. Lottermoser et al., Nature ***430***, 541-544 (2004).
[5]C. W. Nan, G. Liu, Y. Liu and H. Chen, Phys. Rev. Lett., ***94*** 197203 1-4 (2005).
[6]H. Zheng et al., Science ***303***, 661-663 (2004).
[7]J. R. Teague, R. Gerson and W. J. James, Solid State Commum., ***8***, 1073 (1970).
[8]P. Fischer, et al., J. Phys. Solid State Phys.***13*** 1931-1940 (1980).
[9]P. Ravindran et al., Phys. Rev. B***74***, 224412 1-18 (2006).
[10]I. Sosnowska et al., J. Phys.C ***15***, 4835 (1982).
[11]J. Wang et al., Science ***299***, 1719-1722 (2003).
[12]M. M. Kumar, A. Srinvias and S. V. Suryanarayana, J. Appl. Phys., ***87***, 855-862 (2000).
[13]K. Ueda, H. Tabata and T. Kawai, Appl. Phys. Lett., ***75***, 555-557 (1999).
[14] J. S. Kim et al., J. Appl. Phys., ***96***, 468-474 (2000).
[15]D. Lebeugle et al., Phys. Rev. B ***76***, 024116 1-8 (2007).
[16]T. Zhao et al., Nat. Mat. ***5***, 823-829 (2006).
[17]W. Norimatsu and Y. Koyama, Phys. Rev. B***74***, 085113 1-8 (2006).
[18]M. Tanaka and G. Honjo, J. Phys. Soc. Jpn. ***19***, 951-970 (1964).
[19]T. Asada and Y. Koyama, Phys. Rev. B ***70***, 104105 1-5 (2004).

(Received December 8, 2007;Accepted January 31, 2008)